ROLES OF INHIBITORS IN GLOBAL GAS-PHASE COMBUSTION KINETICS

Yuko Saso
National Research Institute of Fire and Disaster

ABSTRACT

Roles of inhibitors in the global kinetics of methane combustion were investigated computationally, by employing the Arrhenius equation to express the global rate constant. When the concentrations of the fuel and the oxidizer in a combustible mixture are kept constant, the global reaction rate is controlled by the flame temperature T_f, the global frequency factor A, and the global activation energy E_a. Changes in A and E_a with the additions of various inhibitors were estimated using the relationship between these parameters and the laminar burning velocity. Inhibitors investigated are He, CO_2, CF_4, CHF_3, C_3HF_7, CF_3Br, CF_3I, NaOH, and $Fe(CO)_5$. The global kinetic parameters were found to vary according to the inhibitors' actions, physical, non-catalytic scavenging, and catalytic scavenging. That is, while He and CO_2 caused negligible changes in both A and E_a, CHF_3 and C_3HF_7 caused significant reduction in A without remarkable changes in E_a. In contrast, CF_3Br, CF_3I, NaOH, and $Fe(CO)_5$ caused noticeable increase in E_a. Although an increase in E_a seems to be a general characteristic of catalytic scavengers, its magnitude showed complicated variation due to many factors including the combustion promotion at higher temperatures and the saturation effect, which is speculated to be dependent on the thermochemistry of key inhibitor species. The maximum increase in E_a with CF_3Br at T_f =2000 K was found to be approximately twice as much as that with $Fe(CO)_5$, which can be attributed to the coexistence of all the key inhibitor species in the CF_3Br-doped flames more equally than those in the $Fe(CO)_5$-doped flames at lower temperatures.

INTRODUCTION

To search for a highly effective suppressant comparable to halons, the behavior of inhibitors in elementary reaction steps of hydrocarbon combustion **has** been extensively investigated [e.g., 1, 2]. **All** the highly effective inhibitors are known to possess catalytic cycles of flame-radical recombination, which are similar to those with the **Br** atom in CF_3Br. Therefore, if one can isolate the catalytic inhibition effectiveness of these inhibitors and determine quantitatively the relationship between the catalytic effectiveness and physicochemical properties of inhibitors, it would assist the search for a new inhibitor species with high performance.

Although several methods have been proposed for quantifying the relative contributions of physical and chemical actions of inhibitors [3-6], few attempts have been performed to isolate the catalytic inhibition effectiveness from other effects including the non-catalytic scavenging effectiveness. The inhibition index **of** Fristrom and Van Tiggelen [7] dealt with the catalytic and non-catalytic scavenging effectiveness separately. It is, however, limited to the comparison **of** the chemical effectiveness between inhibitors at low concentrations where the physical effectiveness is negligible. Sheinson and Maranghides [4] isolated the chemical catalytic effectiveness of CF_3Br using the non-linear behavior of CF_3Br / SF_6 mixtures. In spite of their empirical approach, fundamentals of their method are identical to those of the present work [8].

The classical laminar flame theory derived the following relationship between the laminar burning velocity S_u and the global reaction rate parameters A and E_a:

$$(S_u)^2 = [\text{Fuel}]^m [\text{Oxidizer}]^n \alpha A \exp(-E_a / RT_f) \qquad (1)$$

where α refers to the thermal diffusivity of the mixture and T_f the flame temperature. Therefore, when $\ln\{(\alpha_0/\alpha)(S_u / S_{u,0})\}^2$ is plotted as a function of $1/T_f$, where α, α_0, S_u, and $S_{u,0}$ are respectively the thermal diffusivities and the laminar burning velocities for the inhibited and uninhibited flames with constant fuel and oxidizer concentrations, the slope of the plot represents the global activation energy difference between the inhibited and uninhibited flames, $E_a - E_{a,0}$, and the intercept represents the global frequency factor ratio, A / A_0.

In the previous work, it was indicated that when an inert component of a combustible mixture is partly substituted by an inhibitor, global reaction rate parameters of the gas-phase combustion are increased or reduced systematically according to the inhibitor's actions [8]. CF_3Br, which possesses the catalytic cycles, increases the global activation energy of the methane combustion, while CHF, reduces the global frequency factor without affecting the activation energy. These findings suggest a unified theory of flame inhibition (Figures 1 and 2), in that the negative-catalytic effectiveness and the non-catalytic scavenging effectiveness of inhibitors are defined as the global activation energy difference $E_a - E_{a,0}$ and the global frequency factor ratio A / A_0, respectively. In the present work, roles of inhibitors in the global kinetics of methane combustion were further investigated computationally, to verify the proposed theory of physical and chemical inhibition actions. Roles of inhibitors' kinetics and thermochemistry in the negative-catalytic inhibition will also be discussed.

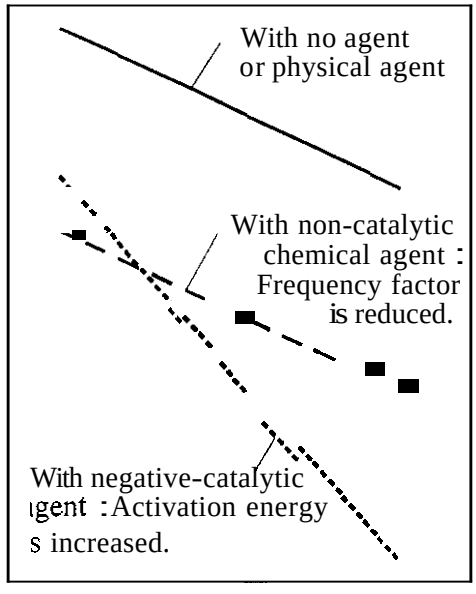

Figure 1. Conceptual Arrhenius plots for global gas-phase combustion reactions of fuel-air mixtures doped with inhibitors that possess various actions.

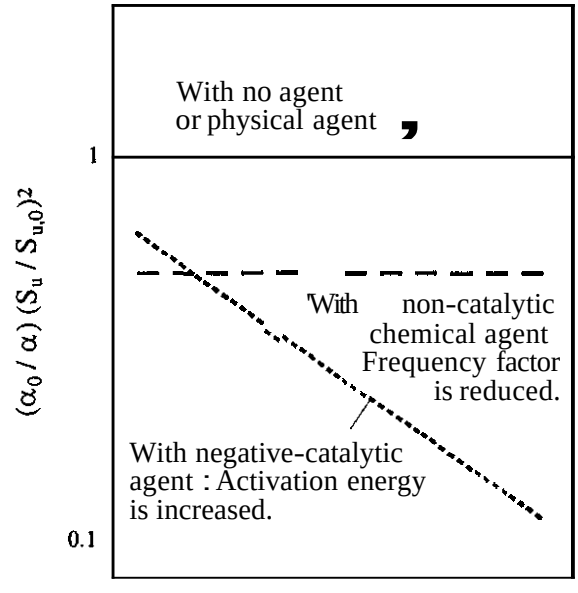

Figure 2. Conceptual plots of $\ln\{(\alpha_0/\alpha)(S_u / S_{u,0})\}^2$ versus $1/T_f$, which can be obtained using the laminar burning velocities determined at various flame temperatures for the inhibited and uninhibited flames with constant fuel and oxidizer concentrations.

NUMERICAL CALCULATIONS

The methane oxidation model was taken from GRI-Mech 2.11 [9] with nitrogen chemistry deleted (31 species and 175 reactions). The inhibitors investigated in this work are He, CO_2, CF_4, CHF_3, C_3HF_7, CF_3Br, CF_3I, NaOH, and $Fe(CO)_5$. The hydrofluorocarbon (HFC) oxidation model for the computation of CF_4-, CHF_3-, C_3HF_7-, CF_3Br-, and CF_3I-containing flames was taken from the work of Williams et al. [10], which is based on the NIST HFC model [11] and the work of Hynes et al. [12], with some rate expressions updated (60 species and 633 reactions). The Brand I chemistry for the computation of CF_3Br- and CF_3I-doped flames was taken from the work of Babushok et al. [13] (Br chemistry: 10 species and 89 reactions; I chemistry: 10 species and 71 reactions). The reaction models of NaOH and $Fe(CO)_5$ were taken from the work of Williams and Fleming [2] and Rumminger et al. [1], respectively. For consistency, the thermochemical data were taken from Ref. 9 for the C/H/O species, for the fluorinated species [10], for the Br- and I-containing species [13], for the Na-containing species [2], and for the Fe-containing species [1].

The laminar burning velocities were computed using CHEMKIN II [14] and the Sandia premixed flame code [15]. The transport coefficients were computed using the computer code of Kee et al. [16]. For consistency, the transport data were taken from Ref. 9 for the C/H/O species, for the fluorinated species [10], for the Br- and I-containing species [13], for the Na-containing species [2], and for the Fe-containing species [1]. The computations were performed for atmospheric pressure flames with unburned mixture temperature of 298.2 K. Computations were carried out in a domain of 85 cm and with windward differencing for the convective terms. To ensure convergence, the mesh resolution was progressively refined until further refinement resulted in a difference of less than 0.5 cm/s in the computed laminar burning velocities.

To determine the inhibitory effectiveness at various flame temperatures, burning velocity computations were performed for mixtures containing 7.5%CH_4, 15%O_2, inert (N_2+Ar) and an inhibitor. The maximum molar percentages of inhibitors were 10% (He and CO,); 6% (CF_4); 5% (CHF,); **3.3%** (C_3HF_7); 1% (CF_3Br), 0.5% (CF_3I), **0.4%** (NaOH), and 0.2% ($Fe(CO)_5$) in the unburned mixtures. At a fixed level of an inhibitor's addition, the flame temperature was varied by manipulating the relative concentrations of nitrogen and argon. Thus, while calculations at the lowest flame temperature were performed with inert being entirely nitrogen, at the highest flame temperature, nitrogen was entirely replaced by argon.

The global frequency factor ratio, A/A_0, and the global activation energy difference, $E_a - E_{a,0}$, were determined using the computed laminar burning velocities according to the following relations. Applying Eq. (1) to the present uninhibited mixtures of 7.5%CH_4-15%O_2-77.5% (N_2+Ar) obtains

$$(S_{u,0})^2 = [CH_4]^m [O_2]^n \alpha_0 A_0 \exp(-E_{a,0}/RT_f) \tag{2}$$

Assuming that the orders m and n are independent of the substitution by inhibitors, **an** inhibited mixture of 7.5%CH_4-15%O_2-77.5% (N_2+Ar+inhibitor) follows an equation,

$$(S_u)^2 = [CH_4]^m [O_2]^n \alpha A \exp(-E_a/RT_f) \tag{3}$$

Thus the following equation is derived from Eq. (2) and **(3);**

$$\ln\left\{\frac{\alpha_0}{\alpha}\left(\frac{S_u}{S_{u,0}}\right)^2\right\} = \ln\left(\frac{A}{A_0}\right) - \frac{E_a - E_{a,0}}{RT_f} \tag{4}$$

Eq. 4 represents that the Arrhenius-type plots (Figure 1) can be converted to the plots of $\ln\{(\alpha_0/\alpha)(S_u/S_{u,0})\}^2$ versus $1/T_f$, (Figure **2).** Here α and α_0 are calculated by the following relations;

$$\alpha = \frac{\lambda}{\rho C_p}, \qquad \alpha_0 = \frac{\lambda_0}{\rho_0 C_{p0}} \tag{5}$$

By plotting the computed laminar burning velocities **in** the form of Figure 2, A/A_0 and $E_a - E_{a,0}$ are determined **as** the intercept and the slope of the line, respectively. If the present theory holds true with an inhibitor, A/A_0 and $E_a - E_{a,0}$ should quantify the chemical effectiveness **as** (a) the non-catalytic scavenging effectiveness and (b) the negative-catalytic effectiveness of the inhibitor, respectively, while the physical effectiveness should he quantified by the remaining parameters in **Eq.** (3), that is, the concentration terms (dilution effect), the thermal diffusivity, and the flame temperature (cooling effect).

RESULTS AND DISCUSSION

Figure 3 shows the computed laminar burning velocity results plotted in the form of Eq. (4) and Figure 2. In Figure 3, the negative of the slope represents $E_a - E_{a,0}$ and the intercept represents A / A_0. It is seen that the difference in major actions among the physical (He, CO_2, and CF_4), the chemical non-catalytic (CHF, and C_3HF_7), and the chemical catalytic (CF_3Br, CF_3I, NaOH, and $Fe(CO)_5$) inhibitors can be fairly well distinguished.

PHYSICAL AGENTS

The plots for the three physical agents (He, CO_2, and CF_4) show negligible slopes and deviations from unity smaller than 20%, indicating insignificant change in both the frequency factor and the activation energy. This is consistent with a general recognition that these agents have no significant chemical effectiveness. With closer observation, however, CO, and CF, show some reduction in the frequency factor. This is more obvious in Figure 4 where the variation of A / A_0, which was determined by neglecting the small $E_a - E_{a,0}$ observed in Figure 3, is plotted as a function of the mole fraction of inhibitors in the unburned mixtures. While A / A_0 for He shows no significant deviation from unity over the entire concentration range investigated, those for CO, and CF, show monotonous decrease with the increase in the mole fraction of inhibitors. The moderate decrease for CO, is mainly attributed to the approximations that Eq. 4 is derived from the simple flame theory with one-step chemistry, and that the flame temperature and the thermal diffusivity are taken from those at the hot boundary and the cold boundary, respectively. Furthermore, about 10% of the total decrease in A / A_0 for CO, is found to be caused by the relatively high third-body collision efficiencies of CO, in the termolecular recombination reactions. Some chemical non-catalytic effectiveness suggested in Ref. 8 should also be an additional cause.

In Figure 4, the decrease in A / A_0 for CF_4 is even more significant than for CO_2. It is known that CF_4 hardly decomposes in methane-air flames while it decomposes completely in the equilibrium mixtures [17, 18]. The present result on CF_4 suggests that the approximation of the adiabatic flame temperature to the reaction temperature of global combustion can cause remarkable errors in the prediction of inhibitory actions, when the difference in an agent's behavior between the flame zone and the equilibrium condition is significant. When the F chemistry is frozen, the reduction in A / A_0 for CF_4 becomes insignificant, as plotted in Figure 4 with a dashed line.

CHEMICAL NON-CATALYTIC AGENTS

By comparison between Figure 2 and the results on CHF_3 and C_3HF_7 in Figure 3, one can easily recognize that these agents act as chemical non-catalytic inhibitors. That is, remarkable reduction in A / A_0 is observed with negligible $E_a - E_{a,0}$. This is consistent with the findings by Westmoreland et al. [17], Linteris and Truett [18], L'Esperance et al. [19], Linteris et al. [20], and Williams et al. [10] that these agents readily decompose in the methane flames and participate in scavenging the reactive flame radicals.

It is also seen in Figure 3 that a slightly positive slope is observed for both CHF_3 and C_3HF_7, indicating a small reduction in the global activation energy. Recognizing that HFCs possess some fuel effect [21], the effect of equivalence ratio variation on the apparent $E_a - E_{a,0}$ was examined by substituting the inert component of the uninhibited mixtures by 1% of CH_4. The results are plotted in Figure 3. The positive slope is observed, demonstrating that an excess fuel causes the apparent activation energy reduction. Therefore, the small negative $E_a - E_{a,0}$ for CHF_3 and C_3HF_7 can be attributed to the combined fuel effect and the reduced inhibitory effectiveness at lower flame temperatures, which was suggested based on both the experimental and the numerical results [8].

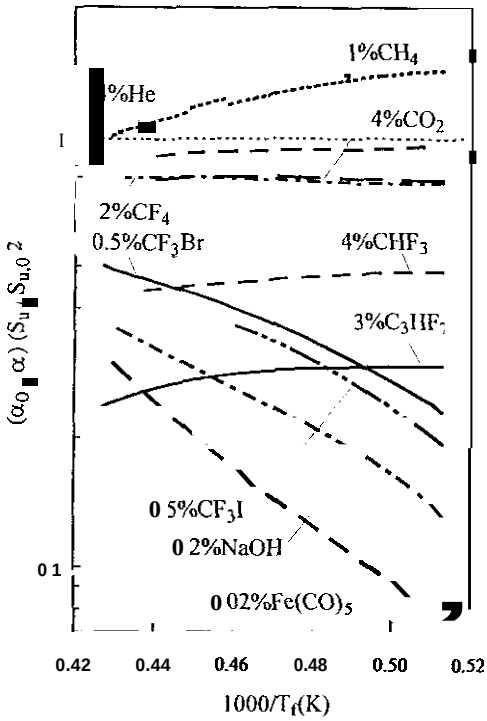

Figure 3. Variation of $\ln\{(\alpha_0/\alpha)(S_u / S_{u,0})\}^2$ as a function of $1/T_f$, calculated using the laminar burning velocities determined at various flame temperatures for the inhibited 7.5%CH_4-15%O_2-77.5% (N_2+Ar+inhibitor) and uninhibited 7.5%CH_4-15%O_2-77.5% (N_2+Ar) mixtures.

The variation of A / A_0 for CHF_3 and C_3HF_7 as a function of the mole fraction of inhibitors in the unburned mixtures was determined by neglecting the small negative $E_a - E_{a,0}$, and plotted in Figure 4. It is found that the reduction in A / A_0 with the increase in C_3HF_7 is approximately twice as significant as that with CHF_3. The global frequency factor is reduced to half with 2% C_3HF_7, while about 4% of CHF_3 is required to achieve the same magnitude of reduction. This is roughly equal to the ratio of the number of F atom in a C_3HF_7 molecule to that in CHF_3.

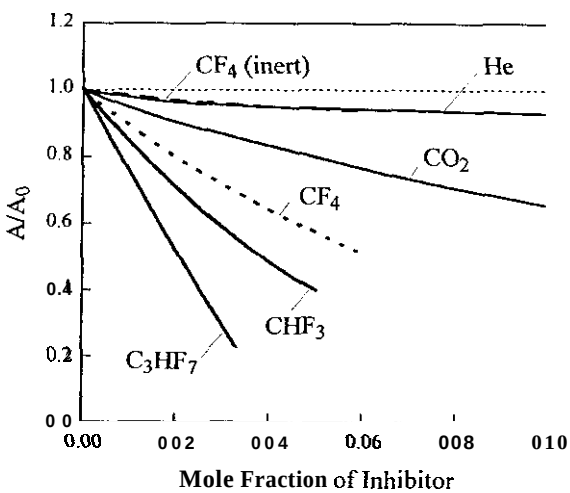

Figure 4. Variation of the global frequency factor ratio as a function of the mole fraction of inhibitor in the unburned mixture, calculated using the laminar burning velocities determined at various flame temperatures for the inhibited 7.5%CH_4-15%O_2-77.5% (N_2+Ar+ inhibitor) and uninhibited 7.5%CH_4-15%O_2-77.5% (N_2+Ar) mixtures.

Noto et al. *[6]* reported that the chemical inhibition effectiveness saturates when the concentration of chemical inhibitor is increased, due to the decrease in the super-equilibrium ratio, $[H]_{max}/[H]_{equil}$, where $[H]_{max}$ and $[H]_{equil}$ are the maximum and the equilibrium concentration of H atom, respectively. In the present study, a slight reduction in the decay of A / A_0 is observed for CHF_3 (Figure 4), but no remarkable reduction is seen for the decay of A / A_0 for C_3HF_7 within the concentration range investigated. The attempt to verify the findings of Noto et al. by computing the laminar burning velocities at larger dosage of inhibitors failed because of a difficulty in computational convergence at higher concentrations of HFCs.

CHEMICAL NEGATIVE-CATALYTIC AGENTS

By comparison between Figure 2 and the results on CF_3Br, CF_3I, NaOH and $Fe(CO)_5$ in Figure **3,** it is easily recognized that these agents act as chemical negative-catalytic inhibitors; **i.e.,** a significant positive $E_a - E_{a,0}$ is observed. This is consistent with the work of Westbrook [22], Babushok et al. [13], Noto et al. [6], Williams and Fleming [2], and Rumminger et al. [1], which suggests that these agents possess catalytic cycles of flame radical recombinations.

Figure 5 shows variations of (a) the global activation energy difference and (b) the laminar burning velocity, both determined at 2000 K, as a function of the molar percentage of inhibitor in the unburned mixture. It is found that the global activation energy differences are almost linearly increased with the increase in the inhibitor concentration, while the laminar burning velocities show the nonlinear decay as pointed out by Noto et al. [6]. In terms of relative levels among the inhibitors, the order of increasing the negative-catalytic effectiveness is found to be CF_3Br, CF_3I, NaOH and $Fe(CO)_5$. This is in agreement with the order of increasing the laminar burning velocity reduction in Figure 5b, demonstrating that the negative-catalytic effect is the dominant action for these agents within the concentration range plotted in Figures Sa and 5b.

The reduction in the laminar burning velocity by CF_3Br and CF_3I must be partly attributed to the non-catalytic scavenging effectiveness due to the CF, moiety. It is, however, difficult to determine A / A_0 directly by extrapolating the curve of Figure **3** for a negative-catalytic inhibitor, because of the noticeable variation of the slope and the narrow temperature range investigated. Thus the results on CF_3Br were compared with those of HBr. Figure Sa shows that the magnitude of the increase in $E_a - E_{a,0}$ has negligible difference between CF_3Br and HBr within the range of the inhibitor concentration lower than 0.8%, indicating that the negative-catalytic effectiveness of CF_3Br is the same as that of HBr. On the other hand, reductions in the laminar burning velocity in Figure Sb differ approximately 10%. Recognizing that the thermal and the dilution effects are eliminated in Figures Sa and 5b, the non-catalytic scavenging effect accounts for the observed difference in the laminar burning velocity reduction between CF_3Br and HBr.

At higher degree of inhibitor doping, $E_a - E_{a,0}$ is found to show striking saturation. Figure Sc shows the saturation of $E_a - E_{a,0}$ computed for $Fe(CO)_5$. At the flame temperature of 2000K, $E_a - E_{a,0}$ increases almost linearly with the increase in the concentration of $Fe(CO)_5$ until 0.02%, at which the negative-catalytic effectiveness saturates suddenly and further increment causes no variation in $E_a - E_{a,0}$. This saturation behavior is in contrast to that of the laminar burning velocity reduction that shows smooth exponential decay. The abrupt saturation was also observed for NaOH, although the inhibitor concentration at the saturation point was **20** times greater than that of $Fe(CO)_5$. CF_3Br did not show the saturation even at the concentration ***50*** times greater than the saturation concentration of $Fe(CO)_5$. As a result, the maximum $E_a - E_{a,0}$ with CF_3Br was found to be approximately twice as much as that with $Fe(CO)_5$. The present results suggest that CF_3Br is twice as powerful a negative catalyst as $Fe(CO)_5$, while the overall chemical inhibition effectiveness is reversed by the A / A_0 term. Attempts to find the saturation points for HBr, CF_3Br, and CF_3I failed due to the difficulty in computational convergence at higher concentrations. It should be noted that the non-catalytic scavenging effectiveness of the CF, moiety in CF_3Br seems to cause a lower saturation concentration than that for HBr, which is implied in Figure Sa as the deviation of $E_a - E_{a,0}$ at higher inhibitor concentrations. This may be due to the additional reduction in the H atom concentration by CF,.

When the results on $Fe(CO)_5$ in Figure 5c are compared between 2000 and 2300 K, it is seen that the abrupt saturation of $E_a - E_{a,0}$ disappears at the higher flame temperature. $E_a - E_{a,0}$ at 2300 K continues to increase monotonously within the concentration range investigated, due to the combustion promotion by excess $Fe(CO)_5$ at higher flame temperatures. That is, $E_a - E_{a,0}$ at 2300 K does not correctly represent the negative-catalytic effectiveness. The present results suggest that special caution should be taken when

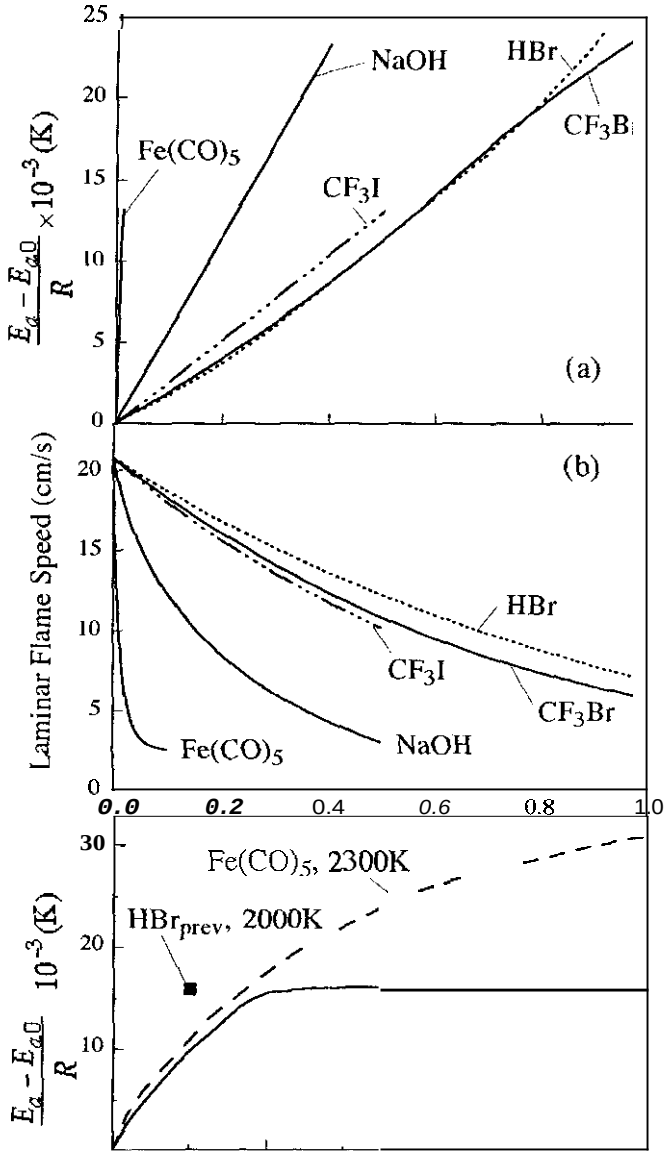

Figure 5. Variations of (a) global activation energy difference and (b) laminar burning velocity, both determined at 2000 K, and (c) global activation energy difference with comparison between 2000 and 2300 K, as a function of the mole fraction of inhibitor in the unburned mixture of 7.5%CH_4-15%O_2-77.5%(N_2+Ar+inhibitor). "HBr_{prev}" denotes the result computed with the reversible perfect inhibition model.

one tries to quantify the negative-catalytic effectiveness of an agent using $E_a - E_{a,0}$, not to be disturbed by the promotion effect that can also be sensitive to the flame temperature **as** the negative-catalytic inhibitory effect.

From the present study, binary use of an inert agent and a powerful negative-catalytic agent is considered to be the most reasonable application of suppressants for gas-phase combustion inhibition. The reasons are as follows: (1) negative-catalytic inhibitors are more effective at lower flame temperatures; (2) the negative-catalytic effectiveness shows an abrupt saturation at a certain concentration and further increment causes only physical effectiveness; and (3) some negative-catalytic inhibitors are known to possess the combustion promotion effect at higher temperatures. An inert agent has two important roles in compensating for these drawbacks of **a** negative-catalytic agent: (1) lowering the flame temperature and **(2)** reducing the concentration of the negative-catalytic agent required for extinguishment. In this way, the present theory on flame inhibition implies potential for next-generation bi-component suppressants.

Rosser et al. [23] pointed out that the strength of the chemical bond in a key scavenger species X–R with the reactive flame radical R is a critical factor in the catalytic inhibition. The present study shows that the thermochemistry that causes relative concentrations of both scavenger species X and X–R to the H atom higher at lower flame temperatures is a dominant factor of a larger $E_a - E_{a,0}$. Figure 6 shows the mole fraction profiles of H and Br atoms in the premixed 7.5%CH_4-15%O_2-76.5%(N_2+Ar)-1%CF_3Br flames with three different flame temperatures. It is seen that while the mole fraction of the H atom decreases significantly with the reduction in the flame temperature, both the peak mole fraction and the equilibrium mole fraction of Br atom show no remarkable sensitivity to the flame temperature. Figure 7 presents the equilibrium mole fractions of H, Br, and HBr as a function of the flame temperature. Both Br and HBr, key species in the catalytic recombination cycles, are quite insensitive to the flame temperature compared with H atom. As a result, the concentration ratios [Br]/[H] and [HBr]/[H] show strong temperature sensitivity. The temperature sensitivity of [Br]/[H] and [HBr]/[H] was found to be even greater than that of the ratio of the rate constant for any dominant chain termination reaction by Br, HBr, or Br_2 to that for the branching reaction. Recognizing that the negative-catalytic effectiveness is defined as the temperature sensitivity of the inhibitory effect $E_a - E_{a,0}$, these results suggest that the thermochemistry of scavenging species is the primary factor of the powerful negative catalysis observed for CF_3Br.

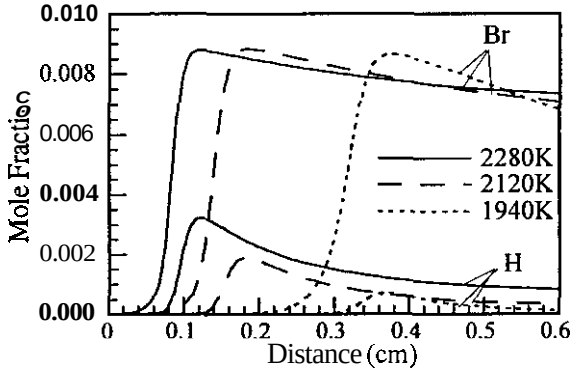

Figure 6. Mole fraction profiles of H and Br atoms in the premixed 7.5%CH_4-15%O_2-76.5%(N_2+Ar)-1%CF_3Br flames with various flame temperatures.

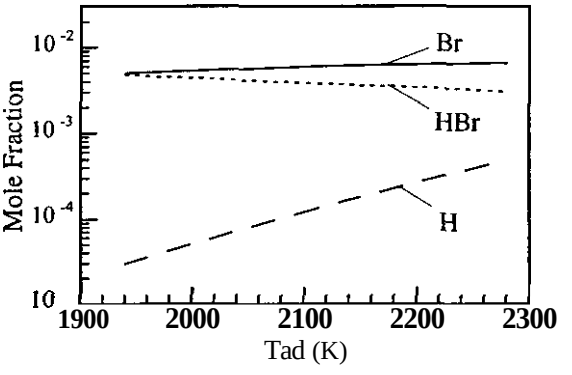

Figure 7. Variation in the mole fractions of H, Br, and HBr at the equilibrium of 7.5%CH_4-15%O_2-76.5%(N_2+Ar)-1%CF_3Br mixtures as a function of the flame temperature.

Figure 8 shows the equilibrium concentrations of H atom and the key scavenger species in the NaOH- and $Fe(CO)_5$-doped flames. The key scavenger species in these flames show noticeable temperature sensitivity. Consequently, the reduction in the flame temperature near 2000 K amplifies the imbalance between the concentrations of the key scavenger species in the catalytic recombination cycles. In particular, the equilibrium in the $Fe(CO)_5$-doped flame is shifted toward $Fe(OH)_2$ significantly with a decrease in temperature. This imbalance in concentration diminishes the efficiency of the catalytic cycles. The stronger temperature sensitivity of the concentrations of key scavenger species results in the catalytic cycles only working in a narrower temperature range, thus causing less flexibility in flame inhibition. The poor flexibility can account for the rapid saturation of the negative catalysis. The order of increasing the maximum $E_a - E_{a,0}$ at T_f=2000K is $Fe(CO)_5$, NaOH, and CF_3Br, which is in good agreement with the order of decreasing the imbalance in the scavenger concentrations.

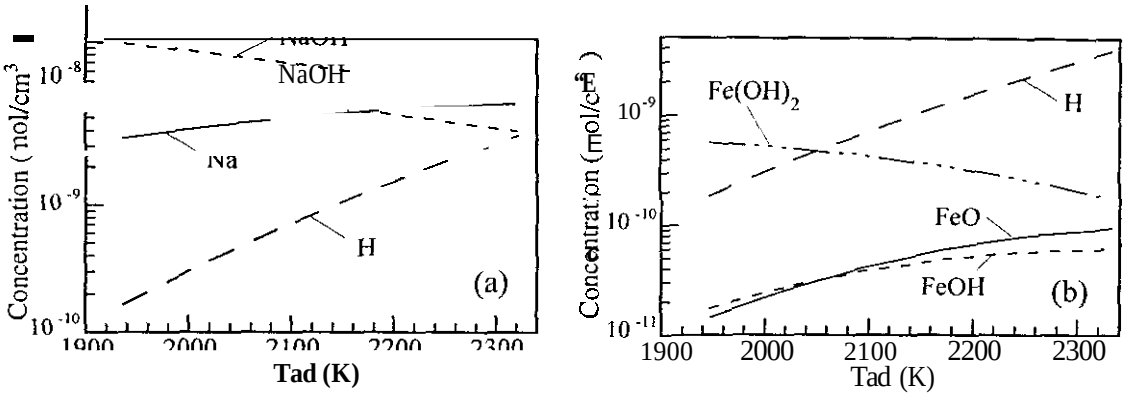

Figure 8. Variation in the concentrations of H atom and the key scavenger species at the equilibrium of 7.5%CH_4-15%O_2-(N_2+Ar) mixtures doped with (a) 0.2%NaOH and (b) 0.01%$Fe(CO)_5$, as a function of the adiabatic flame temperature.

The imbalance between key inhibitor species can be measured by the dissociation energy of the chemical bond between a key inhibitor species X and an active flame radical, H, O, or OH. Rosser et al. [23] pointed out that the bond dissociation energies for effective catalytic species X–H (or X–O or X–OH) should be within a certain range, i.e., not too strong and not too weak. The present study further suggests that this condition should hold over a wide range of temperatures to exhibit powerful negative catalysis.

While the difference in the maximum negative-catalytic effectiveness between inhibitors can be explained by the scavengers' thermochemistry, the significant difference in the slope of the plots in Figure 5a is attributed to the catalytic recombination kinetics, which is demonstrated in Figure 5c. Babushok et al. [24] employed an idealized "perfect inhibitor" to estimate the ultimate limits of chemical inhibition. In the present study, the perfect inhibition model of Babushok et al. was used to verify the role of kinetics in the negative-catalytic effectiveness of HBr and $Fe(CO)_5$. The computations were performed for HBr with an artificial ***reversible*** perfect inhibition model, with the thermochemical data unchanged. The calculated global activation energy difference is plotted in Figure 5c, which is found to be noticeably greater than that for $Fe(CO)_5$. The results demonstrate that the difference in the slope of Figure 5a between HBr and $Fe(CO)_5$ is due to the chemical kinetic processes of the catalytic cycles.

Using E_a–$E_{a,0}$ as a measure of the negative-catalytic effectiveness, the present study has shown the *two* necessary conditions for the negative catalysis: (1) the bond strength in key scavenging species X–R (R=H, O, or OH) should be within certain limits over a wide temperature range, and (2) the kinetics for the catalytic recombination should be fast enough to overcome the chain branching reaction. Further investigation should dig up physicochemical properties of scavenging species that cause the above two conditions.

CONCLUSIONS

The unified theory of flame inhibition, which focuses on the variation of the global reaction rate parameters of gas-phase combustion with the inhibitor doping, was proposed and applied to a wide variety of inhibitors. The chemical non-catalytic, and the chemical negative-catalytic effectiveness of inhibitors were reasonably isolated and quantified by the global frequency factor ratio and the global activation energy difference, respectively. The results suggest that CF_3Br is twice as powerful a negative catalyst as $Fe(CO)_5$ due to the coexistence of all the key scavenging species equally over a wider temperature range.

ACKNOWLEDGMENTS

It is a pleasure to acknowledge beneficial discussions with Dr. Wing Tsang of National Institute of Standards and Technology and Dr. Bradley A. Williams of the Naval Research Laboratory. The kinetic model and related data for NaOH were provided prior to publication by Dr. B. A. Williams. The author also thanks Dr. Valeri Babushok and Dr. Gregory T. Linteris of National Institute of Standards & Technology for providing kinetic models. This work was supported by the Science and Technology Agency of Japan.

REFERENCES

1. Rumminger, M.D., Reinelt, D., Babushok, V., and Linteris, G.T., "Numerical Study of the Inhibition of Premixed and Diffusion Flames by Iron Pentacarbonyl," ***Combustion and Flame,*** 116:207-219, 1999.
2. Williams, B.A., and Fleming, J.W., "Suppression Mechanisms of Alkali Metal Compounds," ***Proceedings,*** Halon Options Technical Working Conference, Albuquerque, NM, pp. 157-169, 1999.
3. Sheinson, R.S., Penner-Hahn, J.E., and Indritz, D., "The Physical and Chemical Action of Fire Suppressants," ***Fire Safety Journal,*** 15:437-450, 1989.
4. Sheinson, R.S., and Maranghides, A., "The Cup Burner as a Suppression Mechanism Research Tool: Results, Interpretations, and Implications," ***Proceedings,*** Halon Options Technical Working Conference, Albuquerque, NM, pp. 19-30, 1997.
5. Saso, Y., Saito, N., Liao, C., and Ogawa, Y., "Extinction of Counterflow Diffusion Flames with Halon Replacements," ***Fire Safety Journal,*** 26:303-326, 1996.
6. Noto, T., Babushok, V., Hamins, A., and Tsang, W., "Inhibition Effectiveness of Halogenated Compounds," ***Combustion and Flame,*** 112:147-160, 1998.
7. Fristrom, R.M., and Van Tiggelen, P.J., "An Interpretation of the Inhibition of C-H-O Flames by C-H-X Compounds," ***Seventeenth Symposium (International)*** on ***Combustion,*** The Combustion Institute, Pittsburgh, pp. 773-785, 1979.
8. Saso, Y., Ogawa, Y., Saito, N., and Wang, H., "Binary CF_3Br- and CHF_3-Inert Flame Suppressants: Effect of Temperature on the Flame Inhibition Effectiveness of CF_3Br and CHF_3," ***Combustion and Flame,*** 118:489-499, 1999.
9. Bowman, C.T., Hanson, R.K., Davidson, D.F., Gardiner, W. C. Jr., Lissianski, V., Smith, G.P., Golden, D.M., Frenklach, M., and Goldenberg, M., GRI Report GRI-97/0020, Gas Research Institute, Chicago, 1997; **http://www.me.berkeley.edu/gri_mech/.**
10. Williams, B.A., L' Espérance, D.M., and Fleming, J.W., "Intermediate Species Profiles in Low Pressure Methane/Oxygen Flames Inhibited by 2-H Heptafluoropropane: Comparison of Experimental Data with Kinetic Modeling," ***Combustion and Flame,*** 120:160-172, 2000.
11. Burgess, D.R. Jr., Zachariah, M.R., Tsang, W., and Westmoreland, P.R., "Thermochemical and Chemical Kinetic Data for Fluorinated Hydrocarbons," ***Prog. Energy Combust. Sci.*** 21:453-529, 1996.
12. Hynes, R.G., Mackie, J.C., and Masri, A.R., "Inhibition of Premixed Hydrogen-Air Flames by 2-H Heptafluoropropane," ***Combustion and Flame,*** 113:554-565, 1998.
13. Babushok, V., Noto, T., Burgess, D.R.F., Hamins, A., and Tsang, W., "Influence of CF_3I, CF_3Br, and CF_3H on the High-Temperature Combustion of Methane," ***Combustion and Flame,*** 107:351-367, 1996.
14. Kee, R. J., Rupley, F. M. and Miller, J. A., "CHEMKIN-II of Fortran Chemical Kinetics Package for the Analysis of Gas-Phase Chemical Kinetics," SAND 89-8009B, Sandia National Laboratories, Albuquerque, NM, 1989.

15. Kee, R.J., Grcar, J.F., Smooke, M.D. and Miller, J.A., "Fortran Program for Modeling Steady-State Laminar One-Dimensional Premixed Flame,'' SAND 85-8240, Sandia National Laboratories, Albuquerque, NM, 1985.

16. Kee, R.J., Warnatz, J. and Miller, J.A., "Fortran Computer Code Package for the Evaluation of Gas-Phase Viscosities, Conductivities, and Diffusion Co-Efficients," SAND 83-8209, Sandia National Laboratories, Albuquerque, NM, 1983.

17. Westmoreland, P.R., Burgess, D.R.F., Jr., Zachariah, M.R., and Tsang, W., "Fluoromethane Chemistry and Its Role in Flame Suppression," *Twenty-Fifth Symposium (International) on Combustion,* The Combustion Institute. Pittsburgh, pp. 1505-I511, 1994.

18. Linteris, G.T., and Truett, L., "Inhibition of Premixed Methane-Air Flames by Fluoromethanes," *Combustion and Flame*, 105:15-27, 1996.

19. L' EspÈrance, D., Williams, **B.A.,** and Fleming, J.W., "Intermediate Species Profiles in Low Pressure Premixed Flames lnhibited by Fluoromethanes," *Combustion and Flame,* 117:709-731, 1999.

20. Linteris, G.T., Burgess, D.R. Jr., Babushok, V., Zachariah, M., Tsang, W., and Westmoreland, P., "Inhibition of Premixed Methane-Air Flames by Fluoroethanes and Fluoropropanes," *Combustion and Flame*, 113:164-180, 1998.

21. Saito, N., Saso, Y., Liao, C., Ogawa, ***Y.,*** and Inoue, ***Y.,*** "Flammability Peak Concentrations of Halon Replacements and Their Functions as Fire Suppressant," in *Halon Replacements: Technology and Science*, ACS Symposium Series 611 (Miziolek, A.W., and Tsang, W., Eds.), The American Chemical Society, Washington, D.C., pp. 243-257, 1995.

22. Westbrook, C.K., "Numerical Modeling of Flame Inhibition by CF_3Br," *Combustion Science and Technology,* 34:201-225, 1983.

23. Rosser, W.A., Wise, H., and Miller, J., "Mechanism of Combustion Inhibition by Compounds Containing Halogen," *Seventh Symposium (International) on Combustion,* Butterworths, London, pp. 175-182, 1959.

24. Babushok, V., Tsang, W., Linteris, G.T., and Reinelt, D., "Chemical Limits to Flame Inhibition," *Combustion and Flame*, 115:551-560, 1998.